ACS APPLIED MATERIALS & INTERFACES

www.acsami.org

Research Article

Armoring the Interface with Surfactants to Prevent the Adsorption of Monoclonal Antibodies

Ankit D. Kanthe, Mary Krause, Songyan Zheng, Andrew Ilott, Jinjiang Li, Wei Bu, Mrinal K. Bera, Binhua Lin, Charles Maldarelli,* and Raymond S. Tu*

Cite This: *ACS Appl. Mater. Interfaces* 2020, 12, 9977−9988

Read Online

ACCESS | Metrics & More | Article Recommendations | Supporting Information

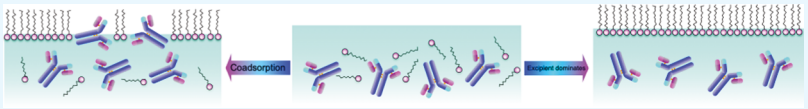

ABSTRACT: The pharmaceutical industry uses surface-active agents (excipients) in protein drug formulations to prevent the aggregation, denaturation, and unwanted immunological response of therapeutic drugs in solution as well as at the air/water interface. However, the mechanism of adsorption, desorption, and aggregation of proteins at the interface in the presence of excipients remains poorly understood. The objective of this work is to explore the molecular-scale competitive adsorption process between surfactant-based excipients and two monoclonal antibody (mAb) proteins, mAb-1 and mAb-2. We use pendant bubble tensiometry to measure the ensemble average adsorption dynamics of mAbs with and without the excipient. The surface tension measurements allow us to quantify the rate at which the molecules "race" to the interface in single-component and mixed systems. These results define the phase space, where coadsorption of both mAbs and excipients occurs onto the air/water interface. In parallel, we use X-ray reflectivity (XR) measurements to understand the molecular-scale dynamics of competitive adsorption, revealing the surface-adsorbed amounts of the antibody and excipient. XR has revealed that at a sufficiently high surface concentration of the excipient, mAb adsorption to the surface and subsurface domains was inhibited. In addition, despite the fact that both mAbs adsorb via a similar mechanistic pathway and with similar dynamics, a key finding is that the competition for the interface directly correlates with the surface activity of the two mAbs, resulting in a fivefold difference in the concentration of the excipient needed to displace the antibody.

KEYWORDS: *monoclonal antibody, excipient, polysorbtate 80, air/water interface, competitive adsorption, X-ray reflectivity, pendant bubble tensiometry*

1. INTRODUCTION

Monoclonal antibodies (mAbs) display an unparalleled selectivity and an exceptionally strong binding affinity for their molecular targets. As a result, mAbs have become leading candidates to be used as therapeutics for the immunological treatment of human disease or the biodiagnostic detection of disease biomarkers. Over the past decade, advances in methods for the production of monoclonal versions of antibodies and improvements in their pharmaceutical purification and production have driven an ever-expanding use of mAbs to treat diseases—including cancer and autoimmune diseases.[1] The critical issue in the administration of mAb biologics is to insure the stability of the formulation in order to preserve the potency and immunogenicity. Understanding the adsorption of therapeutic mAbs at the air/water interface and the competition between the adsorption of excipients and mAb at this interface is critical to the production and administration of the next-generation mAb-based pharmaceuticals. The solution-phase aggregation and precipitation of protein molecules have always been a concern in the pharmaceutical industry.[2,3] Protein aggregates can be generated during the development, production, processing, storage, transportation, and administration of "biologic" therapeutics, thereby decreasing the yields, shortening the shelf-life, and diminishing the desired activity of the proteins.[2,4,5]

The interfacial adsorption and aggregation of protein biologics, in particular mAbs, to the air/water interface is a more recent concern. The interfacial area in the solutions of biologics can lead to the aggregation of proteins at the air/water interface, and the interfacial stress experienced by the proteins under confinement can be exacerbated by surface turbulence induced by mechanical stresses.[6] When mAbs come in contact with an air/water interface, they will adsorb onto the interface by exposing their hydrophobic residues to the gas phase, leading to partial unfolding, structural changes, interfacial aggregation, irreversible adsorption, and recruitment of additional proteins from the solution phase.[7−11] This will result in the formation of protein films that have non-native

Received: December 4, 2019
Accepted: February 4, 2020
Published: February 4, 2020

https://dx.doi.org/10.1021/acsami.9b21979
ACS Appl. Mater. Interfaces 2020, 12, 9977−9988

conformations.[12] This hydrophobically driven adsorption coupled to interfacial stress can cause the conformational degradation of the antibody,[13] where the loss of secondary and tertiary structures can result in diminished activity and affect immunogenicity,[14,15] inhibiting the efficacy of the biologic drugs or engendering side effects during administration.[16,17] Therefore, the quantification and inhibition of the solution phase as well as the interfacial stability of therapeutic drugs are critical in order to increase the production yields and shelf-life of protein-based therapeutics.

In order to circumvent the issues of interfacial protein adsorption, the pharmaceutical industry uses a multicomponent formulation that includes surface-active excipients,[18,19] which compete with the protein for adsorption onto the surface. With coadsorption, both the surfactant and protein can coexist on the surface, and the presence of the adsorbed excipient can also interact with the protein and lead to its unfolding. The major objective is to use excipient concentrations large enough so that the rate of excipient transport to the surface is much greater than that of the protein, effectively preventing the protein from being adsorbed. An additional effect in the competitive adsorption process is that surfactants can form complexes with proteins in solution.[20] This complexation tends to stabilize the proteins and prevents their adsorption to the surface.

The most commonly used nonionic excipients in biopharmaceutical formulations are polysorbate 20 and 80 (or Tween 20 and 80).[21] There have been studies in the literature on protein−surfactant adsorption onto the air/water interface using surface tensiometry[22−25] and interfacial rheology methods.[18,26−28] Generally, these studies have found that globular proteins such as bovine serum albumin (BSA) will not be able to compete for area at the air/water interface when in competition with Tween 20 concentrations higher than the critical micelle concentration (cmc).[29] For the case of mAb proteins, there is a paucity of studies on the competitive adsorption of mixed protein−polysorbate systems.[30,31] These earlier efforts only used dynamic tension measurements to study the competitive adsorption, and the conclusions relied only on the concentration of the surfactant at which the tension curve of the mixture was identical to the tension curve of the pure surfactant solution (at the same concentration). This concentration defined the surfactant concentration necessary for the surfactant to dominate the adsorption process. Unfortunately, these ensemble average tools do not yield a molecular-scale mechanistic understanding of the competitive adsorption process.

In order to resolve molecular mechanisms, X-ray measurements can be employed to reveal the structural features, surface coverage, and characterize the two-dimensional organization of the adsorbed proteins at the air/water interface, giving a near-atomic level structural information at the liquid−vapor interface.[32,33] We have chosen X-rays over neutrons in view of a larger magnitude of the wave vector transfer, Q_z values (up to 0.60 $Å^{-1}$ in our case as opposed to around 0.20 $Å^{-1}$ for neutrons), resulting into more detailed information.[11,14,34] X-ray reflectivity (XR) has enabled molecular-level details for the protein adsorption and their preferential orientations at the solid/water interface.[14,35−37] XR at the air/water interface allows one to quantify both the surface concentrations and structural details of the proteins and excipients.

The aim of this work is to explore the molecular-scale competitive adsorption process between surfactant-based excipients and antibody proteins. The potential possibilities for the mAb and excipient adsorption system to the air/water interface are shown in Figure 1. In this "race" to the interface,

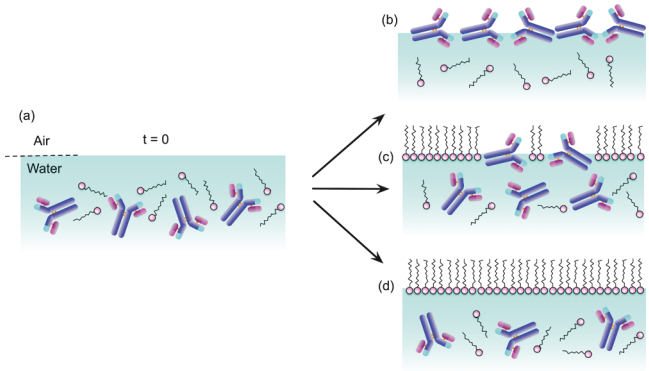

Figure 1. Three outcomes for mAb and excipient adsorption to the air/water interface. (a) Initially, adsorption occurs as the two components, mAbs and surfactants, compete for free surface space. (b) mAbs preferentially occupy the interface because of irreversible adsorption. (c) Coadsorption of mAbs and surfactants occurs governed by a balance of diffusion and dynamic adsorption. (d) Surfactants inhibit mAb adsorption because of the higher surface activity of the surface-active molecule.

we will determine the critical concentrations of the excipient required to prevent the adsorption of the two mAbs at the air/water interface, highlighting the role of solution-phase stability in the critical concentration of the excipient. To quantify this surface activity, we use pendant bubble tensiometry on single-component systems, revealing the dynamics of the adsorption process of the excipient alone and mAb alone, defining the surface concentrations and the area per molecule. Subsequently, we explore two-component systems to quantify the dynamics of coadsorption of the antibody−excipient system. Tensiometry, taken together with XR, allows us to unravel the surface population of the molecules and mechanistically understand the competition of the mAb and the excipient in the adsorption process as they race to the interface. We find the presence of mAbs at the interface even at concentrations where tensiometry suggests the complete displacement of mAbs by surfactant excipients. This finding highlights the complex molecular interactions present in multicomponent systems at the air/water interface. Moreover, the ability of surfactants to displace mAbs at the interface is highly sensitive to the mAbs surface activity.

2. MATERIALS AND METHODS

2.1. Materials. mAb-1 and mAb-2 belong to the IgG1 and IgG4 family having a molecular weight of 145 526.44 and 146 464.92 Da, respectively. The mAbs are provided by Bristol Myers Squibb, New Brunswick, USA, and are supplied as a stock solution of 5 mg/mL for mAb-1 and 10 mg/mL for mAb-2 in 20 mM histidine buffer at pH 5.8. The measured extinction coefficients for mAb-1 and mAb-2 at 280 nm are 1.75 and 1.59 mL mg^{-1} cm^{-1}, respectively. The stock solutions are stored under −80 °C and are thawed and diluted using histidine buffer at pH 5.8 at the same ionic strength of 20 mM. Polysorbate 80 (average molecular weight 1310 g/mol) is of reagent grade and donated by Bristol-Myers Squibb, New Brunswick, and was used as received. Histidine and NaOH for pH adjustments are purchased from Sigma-Aldrich and Fisher Scientific and are used without any further purification. Mixed mAb−polysorbate 80 solutions are prepared from the stock solution of the excipient in

https://dx.doi.org/10.1021/acsami.9b21979
ACS Appl. Mater. Interfaces 2020, 12, 9977−9988

20 mM histidine buffer. The mAb solutions and the buffer are filtered using 0.22 μm polytetrafluoroethylene filters. Milli-Q ultrapure water (Millipore Corp., resistivity 18.2 MΩ cm) is used for dilution of samples.

2.2. Dynamic Tension Measurements. Dynamic surface tensions were measured using a pendant bubble tensiometer (Attension Theta, Biolin Scientific, Stockholm, Sweden). The bulk solution of the antibody and (or) excipient is placed in a quartz cell arranged in an optical train between a light source and a camera. An inverted 16 gauge hollow needle is positioned in the solution, and a pendant bubble (volume ≈ 22 μL) is formed at the tip of the needle by connecting the needle via Teflon tubing to a Hamilton gas-tight syringe loaded in a syringe pump (PhD, Harvard Apparatus) and programming the pump to push air through the tubing and the needle. Dynamic tensions, as the excipient and antibody adsorb to the surface, are obtained by recording the changing bubble shape because of the tension relaxation as a function of time and obtaining the tension from the recorded images using the Young−Laplace equation. The bubble images were recorded for 1.0×10^4 s at a frame rate of 6.5 fps for the first 5.0×10^3 s and at a frame rate of 3.5 fps for the remaining time. Before each experiment, the syringe, needle, and quartz cell were cleaned with deionized (DI) water, followed by sonication for 60 min. All measurements were performed at room temperature (20 ± 3) °C. Each experiment was started by measuring the surface tension of the clean air/water interface using DI water and verifying that the tension was in the range of (72.5 ± 0.3) mN/m, the reference value of water at 20 °C. The error bars are the standard deviations of three experimental results.

2.3. Subphase Exchange Measurements. Experiments exchanging the subphase of pendant drops formed using a tensiometer are undertaken with a coaxial capillary needle (Rame-Hart Instrument Co., Succasunna, USA). This needle allows a drop to be first formed by infusion of a liquid through the outer capillary. The drop liquid is then exchanged by a simultaneous withdrawal of the liquid through the outer capillary and infusion of a second liquid through the inner capillary. Specifically, a drop containing mAb (0.5 mg/mL) is formed using the outer capillary and the dynamic surface tension is recorded as a function of time until 5.0×10^3 s. The drop subphase is then exchanged with either the buffer or PS80 by withdrawing the mAb solution and replacing it with either the fresh buffer or surfactant-only solution. The withdrawal and infusion are maintained at equal rates so that the drop volume (and surface area) remains constant during the exchange. The exchange is undertaken for a period of time that allows the drop to be flushed with approximately 60-fold of drop volume to ensure that the subphase has been completely exchanged. This exchange is completed between 5.0×10^3 and 6.0×10^3 s, after which the dynamic tension is recorded following the exchange up to 1.0×10^4 s. The flow rates for the exchange and the number of drop volumes replaced were determined using sodium dodecyl sulfate (SDS) solutions as a control. Drops of micellar solutions of SDS were formed and allowed to come to an equilibrium tension, after which exchange was undertaken using pure water. The tension recorded during the exchange showed that the surfactant desorbed off the surface. The number of exchange volumes used in the mAb exchange experiments is equal to the number observed to allow the tension of the SDS drop to return to the clean surface tension value.

2.4. XR Measurements. All XR measurements are conducted at NSF's ChemMatCARS, station 15 ID-C experimental hutch at the Advanced Photon Source in Argonne National Laboratory (Argonne, IL).[32,38,39] An incident X-ray beam of wavelength λ = 1.24 Å is used, and data are collected using a Pilatus 100 K area detector. A custom-built mini-Teflon trough of 11 cm × 5 cm × 0.2 cm is machined and used as an insert to fit the existing XR setup. The sample volume required for the XR measurement is 22 mL. The formation of this liquid layer and its associated planar interface is considered to be $t = 0$ for the adsorption process. The trough is in a chamber, and after the trough is filled, the chamber and the hutch room enclosing the X-ray beam are closed. This process takes approximately 20 min. Before each XR measurement, the chamber was purged with helium to maintain the oxygen level to be <1 % (v/v) in order to reduce the beam damage and the background scattering, which takes an additional 30 min. A scan of the surface then takes 40 min. Hence, before the first scan can begin, a minimum of approximately 5.4×10^3 s have elapsed from the moment the air/liquid interface of the trough was formed. All the X-ray data reported correspond to the adsorption process at approximately 9.0×10^3 s from the formation of the clean interface. The XR data are measured as a function of incident angle over the wave vector transfer $Q_z = (4\pi/\lambda)\sin(\alpha)$ along the surface normal to cover the range $0.016 < Q_z < 0.6$ Å^{-1}. The position of the sample is shifted periodically perpendicular to the beam, to avoid any radiation damage. All the measurements are carried at room temperature (20 ± 3) °C. The details for the XR data analysis are provided in the Supporting Information.

3. RESULTS AND DISCUSSION

3.1. Dynamic Surface Tension Relaxation Measurements. The relaxations in dynamic surface tension for the single-component adsorption of the polysorbate 80 (PS80) excipient or the mAbs from bulk solution to an initially clean air/water interface are shown in Figure 2. The single-component case is presented first, as these will function as reference curves for the competitive adsorption from the mixed solutions of mAb and PS80. Figure 2b gives the dynamic tension reductions as measured using a pendant bubble tensiometer (Figure 2a, Materials and Methods) for adsorption from pure PS80 solutions of increasing bulk concentration over

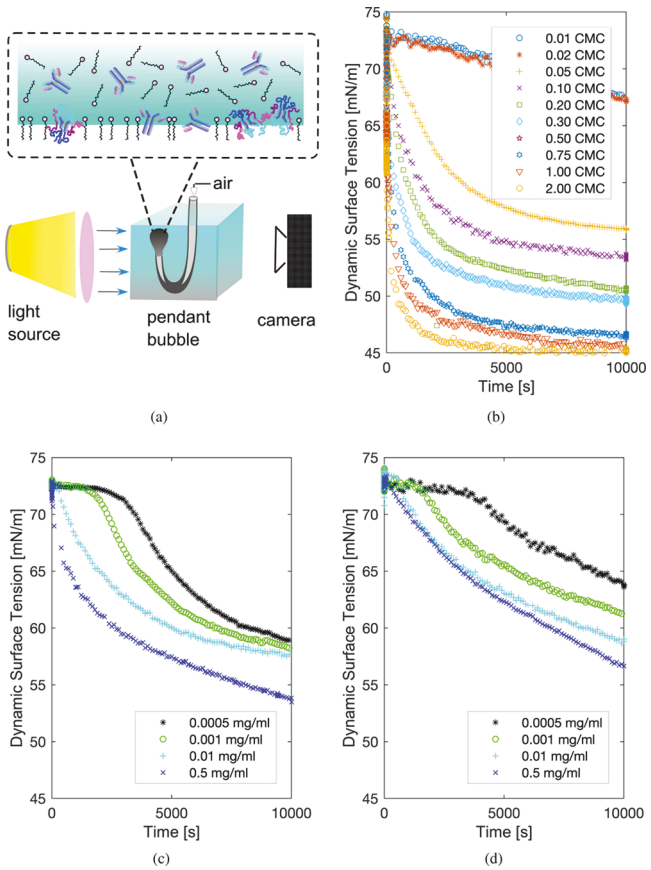

Figure 2. Dynamic surface tension relaxation measurements for single-component solutions of the excipient, polysorbate 80, and the mAbs: (a) Pendant bubble is inflated in a surfactant and (or) antibody bulk solution, and the changes in the bubble shape as the amphiphilic molecules adsorb and those in the tension are recorded. Surface tension relaxations for (b) PS80, (c) mAb-1, and (d) mAb-2.

https://dx.doi.org/10.1021/acsami.9b21979
ACS Appl. Mater. Interfaces 2020, 12, 9977−9988

the time range of 1.0 to 1.0 × 10^4 s. The timescales for the relaxation follow the usual observation for low-molecular-weight surfactants, and increased bulk concentration increases the relaxation rate as the flux of the surfactant to the initially clean interface becomes larger with the increasing bulk concentration.

A plot of the equilibrium tension obtained from the plateau values in the longtime dynamic tension as a function of the logarithm of the bulk concentration is constructed (Supporting Information, Figure S1) and it is demonstrated that the higher the bulk concentration, the smaller would be the equilibrium tension. Based on this, the cmc for PS80 was found to be around 0.012 mM. This is also evident in the dynamic tensions shown in Figure 2b. For large enough concentrations, the equilibrium tension does not change with the bulk concentration (in Figure 2b), and this behavior is indicative of the formation of micellar aggregates in the bulk that come into equilibrium with the surfactant monomer, reducing the thermodynamic driving force for adsorption onto the surface.[40,41]

Figure 2c,d shows the measured reduction in dynamic tension over an interval of 1.0 s to 1.0 × 10^4 s as either mAb-1 (c) or mAb-2 (d) adsorbs from a bulk solution without the surfactant to the initially clean air/water interface. The antibody concentration is between 5.0 × 10^{-4} and 5.0 × 10^{-1} mg/mL. The profiles for the tension reduction for these antibodies are similar in form to the relaxations measured for other proteins such as BSA, lysozyme, β-casein, and other antibodies.[16,42−45] First (as with the low-molecular-weight surfactants), the greater the bulk concentration, the greater would be the tension reduction. Second, for the lowest bulk concentrations, 5.0 × 10^{-4} to 1.0 × 10^{-3} mg/mL, an early induction period in the tension appears in which the surface tension remains approximately equal to the value for the clean air/water interface (≈72.3 mN/m) before decreasing rapidly. As seen in Figure 2c,d, the length of time for the induction period decreases with an increasing bulk concentration. At a high concentration, the plateau disappears from the profile and the tension reduction begins immediately. Third, the plateau behavior in the tension for long times is not evident; examinations at longer times indicate that the tensions continue to monotonically decrease and never approach an equilibrium value, with the tensions at all concentrations appearing to merge. This behavior is indicative of the irreversible adsorption of the mAbs to the surface.[46,47]

Although the surface activity of the two mAbs cannot be compared based on the plots of the equilibrium tension as a function of bulk concentration, differences in their surface activity can be clearly observed by comparison of their dynamic tension relaxations. This difference reflects the fact that the flux of the protein to the surface is larger for mAb-1 relative to mAb-2. As the bulk concentrations are the same, the difference is due to the surface affinities that maintain smaller sublayer concentrations for mAb-1 relative to mAb-2 and hence a larger diffusive driving force of mAb-1 to the surface.

The higher surface activity of mAb-1 relative to mAb-2 can be rationalized based on an examination of their spatial aggregation propensity score (SAP). SAP computes the exposed hydrophobicity of the antibody surface by atomistic simulations of the mAb molecule with explicit water molecules.[48] A larger SAP score indicates more surface hydrophobic patches. For mAb-1 and mAb-2, the scores are 38 and 15, respectively, indicating that mAb-1 has more surface hydrophobic patches and therefore a higher surface activity, as is clear from the dynamic tension data.

To investigate the competitive adsorption of PS80 and mAb to a clean air/water interface, dynamic tension relaxations are measured for adsorption to the surface from mixed solutions containing both the antibody and the surfactant excipient. For the purposes of this comparison, a single concentration of the antibody is chosen, and the concentration of the excipient is varied to examine the competitive adsorption. In the administration of mAbs, dosages are typically large (order 10 to 10^2 mg/mL); so, the adsorption timescale of the antibody alone will be fast (<1 s). However, to examine the coadsorption dynamics with the time resolution of the pendant bubble tensiometer, which is of the order of 1 s, a concentration of 5 × 10^{-1} mg/mL is selected. This mAb concentration reflects the IV administration fluid where the concentrated protein solutions are diluted to approximately 1000-fold (1 × 10^{-1} mg/mL).[49,50] Although this concentration is not as large as in clinical practice, the timescale for the mAb relaxation is slow enough (order 10^3 s) to observe the effect of the excipient on the relaxation profile.

Figure 3a,b shows the results for the dynamic tension relaxations for the simultaneous adsorption from a mixed

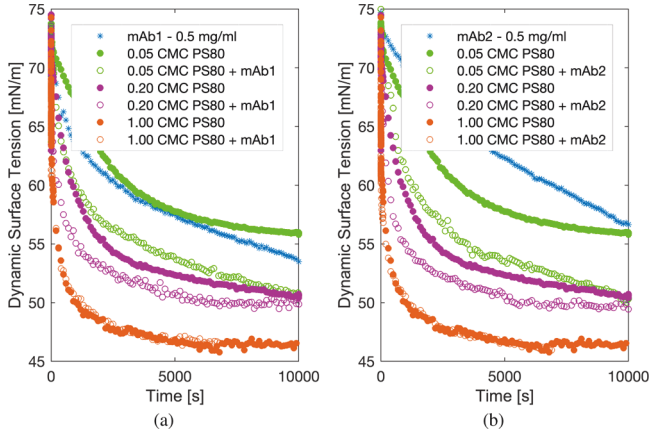

Figure 3. Reduction in surface tension as a solution of mAb at a fixed concentration (0.5 mg/mL) and increasing concentrations of the excipient, polysorbate 80 (0.05, 0.20, and 1.0 × cmc), adsorbs to the pendant bubble interface: (a) mAb-1 and PS80 and (b) mAb-2 and PS80 shown in open markers. The relaxation curves corresponding to a solution of pure mAb (at 0.5 mg/mL) and pure polysorbate 80 in filled markers (0.05, 0.20, and 1.0 × cmc) are shown for comparison with the relaxations for the mixed mAb/excipient system.

solution of mAbs at the fixed concentration of 0.5 mg/mL and PS80 (at increasing concentrations from 0 to 1.0 × cmc). The figures clearly show that for particular fixed PS80 concentrations equal to 0.05 × cmc and 0.2 × cmc, the dynamic tension relaxation profile in the presence of either of the mAb lies below the relaxation curve for adsorption from a solution with only PS80 (at the same concentration). This indicates that, in the mixed layer, the antibody is present and contributes to the surface tension reduction. For example, for solutions with the concentration of excipient equal to 0.05 × cmc and mAb-1, the surface tension value at 10^4 s is 51 mN/m as compared to 57 mN/m for the tension for a solution with only excipient. However, this difference in the relaxation profiles decreases with an increase in the PS80 concentration. For the largest PS80 concentration, 1.0 × cmc, the presence of the

https://dx.doi.org/10.1021/acsami.9b21979
ACS Appl. Mater. Interfaces 2020, 12, 9977−9988

protein appears to have no effect on the relaxation as the tension relaxations for bulk solutions with and without antibodies are identical. Note that although the surface activity of mAb-2 is less than that of mAb-1 (Figure 2c,d), there appears, in terms of tension relaxations, to be little difference in the competitive behavior of PS80 with mAb-2 as compared to PS80 with mAb-1.

Using the dynamic tension measurements, others have observed the dominance of surfactants over proteins at air/water interfaces (see Table 4 in Section 4).[22−24,31] This behavior can be explained by the fact that the flux of the surfactant to the surface outscales that of the protein when the concentration of the surfactant becomes large enough, and the surfactant populates the surface as a monolayer excluding the protein at the interface. For the dynamic tension measurements for the competitive adsorption of mAb-1 and mAb-2 at 0.5 mg/mL with PS80, if the concentration of the mAbs were increased, then their rate of adsorption to the surface would increase and a larger concentration of PS 80 (in excess of 1.0 × cmc) would be necessary to exclude the mAbs from the surface.

3.2. Subphase Exchange Measurements. The continuous reduction in the dynamic tension relaxation of solutions containing only mAbs, as recorded by the pendant bubble tensiometer (Figure 2c,d), indicated the irreversible adsorption of the mAbs to the surface. To understand under what circumstances these already adsorbed mAbs can be displaced from the surface, subphase exchange experiments are undertaken for mAb-1 using a coaxial needle to form pendant drops whose subphases can be replaced. The schematic and timescale of the exchange experiments are shown in Figure 4a. As a baseline, the dynamic surface tension relaxation of a drop containing pure mAb-1 (0.5 mg/mL) was measured for 1.0× 10^4 s, and the recorded reduction in tension (Figure 4b) is similar to the result for the adsorption to a bubble interface (Figure 2c). A second experiment is then undertaken in which a drop of pure mAb-1 is exchanged with pure histidine buffer after 5.0 × 10^3 s of adsorption. After the exchange period, the tension continues to relax slowly and, importantly, does not return after a long time to the tension of a clean surface. This indicates that the mAb molecules, once adsorbed onto the surface, do not desorb back into the bulk phase, providing support to the assumption that the mAbs are irreversibly adsorbed to the surface. The slow decrease in the surface tension value after the exchange can be attributed to the slow unfolding or rearrangement of the already adsorbed mAb molecules at the air/water interface.

In order to understand if a surfactant can displace mAb molecules already adsorbed onto the air/water interface, exchange experiments were undertaken in which drops from a pure mAb-1 solution (0.5 mg/mL) are formed and the mAbs are allowed to adsorb for 5.0 × 10^3 s. After establishing the mAb adsorption to the surface, the drop volume is replaced with either 0.05 × cmc or 1.0 × cmc PS80 solution, and the tension is recorded to be 1.0 × 10^4 s (Figure 4b). When the drop volume is exchanged with the surfactant at a concentration of 0.05 × cmc, the tension observed after the exchange continues to slowly decrease until a plateau value approximately equal to 54 mN/m is achieved. Importantly, this value is lower than the steady equilibrium tension of the pure surfactant solution at 0.05 × cmc (≈57 mN/m), as obtained from the pendant bubble tensiometry data (Figure 2b). This result suggests that the already absorbed mAb molecules

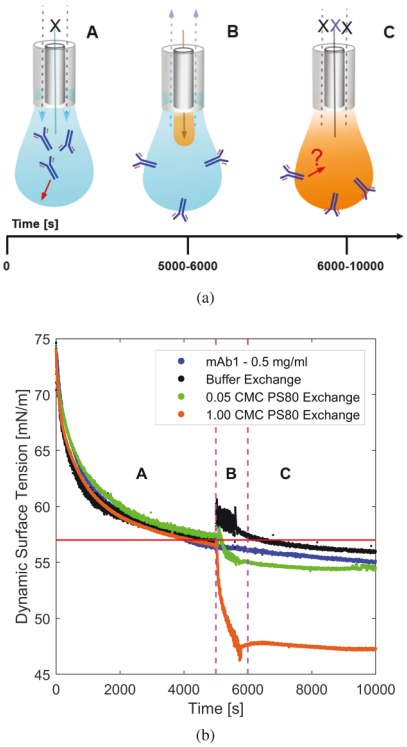

Figure 4. Subphase exchange measurement: (a) timeline of the exchange experiments. The mAb solution is represented by blue color, and the orange represents either the histidine buffer or PS80 solution for the exchange process. The dynamic tension of mAb solution is recorded for 5.0 × 10^3 s (A), followed by the exchange process with the histidine buffer or PS80 between 5.0 × 10^3 s and 6.0 × 10^3 s (B). The tension measurement continues up to 1.0 × 10^4 s after the exchange process (C). (b) Exchange experiment of mAb-1 with the buffer (black), 0.05 × cmc PS80 (green), and 0.10 × cmc PS80 (orange). The blue curve represents the mAb-1 dynamic tension profile using the pendant drop method for comparison. The magenta dashed lines represent the time for the exchange experiments. The solid straight line represents the equilibrium surface tension value of the 0.05 × cmc PS80 solution.

remain on the surface, and the reduction in tension is due to the slow relaxation of the adsorbed mAb and the adsorption of the PS80 to the surface. If the protein had been completely (or significantly) displaced, the surface tension should have approached the value of 57 mN/m (indicated by the solid straight line in Figure 4b).

A significantly different result is obtained when the subphase exchange is undertaken with a PS80 solution with a concentration of 1.0 × cmc. In this case, the tension continues to decrease after the exchange until it plateaus at an equilibrium value (≈46 mN/m) (Figure 4b). This value corresponds to the equilibrium tension of a solution of PS80 with a concentration of 1.0 × cmc, as shown in Figure 2b. This suggests that the surfactant has removed the already adsorbed mAbs from the surface at the cmc concentration. For this case, removal is possible because the mAbs can desorb into the bulk micelles present at the interface, in much the same way that micellar solutions remove hydrophobes from surfaces.

However, as noted in the Introduction section, when the relaxations of the mixed and pure surfactant systems do overlap, proteins can still be bound to the surface as a second layer or as multilayers attached underneath the surfactant monolayer, minimally affecting the surface tension of the

https://dx.doi.org/10.1021/acsami.9b21979
ACS Appl. Mater. Interfaces 2020, 12, 9977−9988

interface. Alternatively, the concentration of mAb at the surface may be small enough (because the rapid PS80 adsorption outscales the mAb adsorption) that it does not affect the surface tension. Therefore, we use XR to directly measure the adsorbed densities of the antibody and the surfactant to understand the molecular organization, particularly in the excipient concentration range where the tension relaxations overlap.

3.3. XR Measurements. Measurements of XR from an air/water interface with the adsorbed mAbs and (or) excipients are obtained in an arrangement (Figure 5a) in which the X-rays

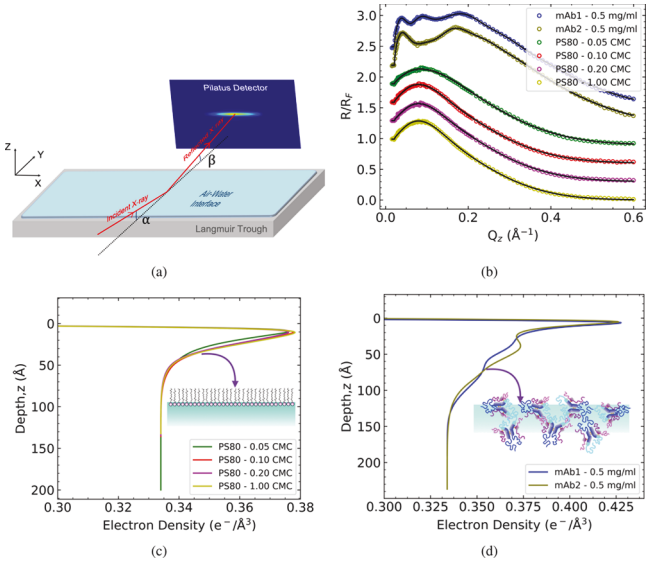

Figure 5. XR measurements from the adsorbed layers at the air/water interface derived from adsorption from single-component bulk solutions of mAbs or excipient. (a) XR measurement with the bulk solution in a trough. The X-ray beam is incident on the air/water interface at an angle α, in the y-direction. For the XR data measurement, $\alpha = \beta$. (b) Normalized X-ray reflectivity, R/R_F (symbols), as a function of the wave function Q_z and Parratt model fits (solid line) for mAb-1 (0.5 mg/mL), mAb-2 (0.5 mg/mL), and PS80 (0.05, 0.10, 0.20, and 1.0 × cmc). XR data for mAbs show multiple peaks for $Q_z < 0.2$ Å, whereas PS80 shows a single peak in this range. The upper five XR curves are shifted for clarity, although $R/R_F \rightarrow 1$ as $Q_z \rightarrow 0$ for all measurements. The corresponding electron density determined by the fits in (b) for the adsorption layers of PS80 alone (c) and mAb-1, mAb-2 (alone) (d). The EDP of mAbs has two peaks instead of a single peak as observed for PS80.

are incident at an angle α onto the planar air/water interface of a liquid film situated in a rectangular trough. The liquid layer consists of bulk solutions of mAbs and (or) the excipient that are poured into the trough, and the adsorbed layers of the antibody and excipient form by adsorption from the layer to the surface. The reflectivity R is measured as a function of the incident angle α, and the scans are reported as the normalized reflectivity R/R_F as a function of the wave vector transfer $Q_z = (4\pi/\lambda)\sin(\alpha)$, where λ is the wavelength of the incident X-ray and $R_F(Q_z)$ is the Fresnel reflectivity from an ideally smooth air/water interface. The reflectivity data can be fit, using the Parratt method,[32,51] in which the electron density at the interfacial region is divided into multiple slabs of different thicknesses and electron densities to calculate the reflectivity curve and to compare with the experimental reflectivity. At the end of the fitting, the electron density profile (EDP) as a function of depth z is obtained (for details, see the Supporting Information).

The reflectivity from the adsorbed layers consisting of only the excipient or antibody is reported in Figure 5b. The figure shows the normalized reflectivity (R/R_F) and the Parratt fit of the reflectivity from the adsorbed layers obtained from the bulk solutions of only mAb-1 or mAb-2. The bulk concentration of 0.5 mg/mL is used as the antibody concentration matching the dynamic tension competitive protein/excipient adsorption experiments. The figure also shows the reflectivity from the adsorbed layers obtained from the bulk solutions containing PS80, for the concentration range 0.05 × cmc to 1.0 × cmc, the range used in the competitive adsorption experiments. The excipient reflectivity data show only a broad maximum for the concentration range studied as opposed to three maxima peaks for mAb-1 and two maxima peaks for mAb-2.

Figure 6 shows the reflectivity data and the corresponding EDP for the adsorbed layers formed by the competition in

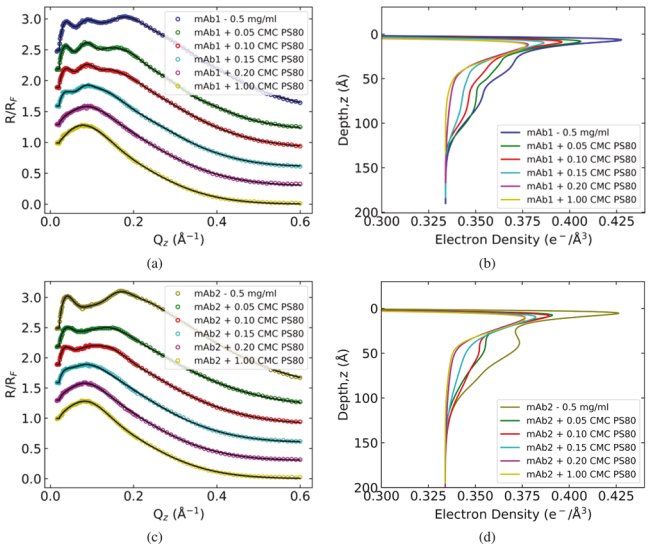

Figure 6. XR measurements from the adsorbed layers at the air/water interface derived from competitive adsorption from the mixed solutions of mAb and excipient. (a) X-ray reflectivity, R/R_F (symbols), as a function of Q_z and Parratt model fits (solid line) for mAb-1 (0.5 mg/mL) and PS80 at increasing concentrations (0.05, 0.10, 0.20, and 1.0 × cmc). The upper five XR curves are shifted for clarity. (b) EDPs as a function of depth for the mAb-1/excipient mixed surface layers, as determined from (a). (c) R/R_F (symbols) as a function of Q_z and Parratt model fits (solid line) for mAb-2 (0.5 mg/mL) and PS-80 (0.05, 0.10, 0.20, and 1.0 × cmc). (d) EDPs as a function of depth for the mAb-2/excipient mixed surface layers, as obtained from (c).

adsorption between the mAbs (at a fixed concentration, 0.5 mg/mL) and PS80 at varying concentrations from the bulk solution. The excipient concentration was varied, so that the resulting mixture volume had 0.05, 0.10, 0.15, 0.20, and 1.0 × cmc of the excipient. For the competitive adsorption between mAb-1 and PS80, the reflectivity curves make clear that as the concentration of the excipient increases, the three maxima—characteristic of the adsorption of mAb-1—converge into a single broad peak, indicating excipient-like behavior. The intensity of the peaks in mAb-1 begins to decrease at 0.05 × cmc, demonstrating the mixed adsorption layers and corroborating observations from the pendant bubble tensiometry data. (More detail about this is presented by overlapping

https://dx.doi.org/10.1021/acsami.9b21979
ACS Appl. Mater. Interfaces 2020, 12, 9977−9988

the XR curves; see Figure S2 in the Supporting Information.) Similar information can be inferred from the EDP shown in Figure 6b, where mAb-1 showed more than one peak in the EDP as opposed to a single peak for the excipient. As the PS80 concentration reaches 1.0 × cmc, the reflectivity curve for this adsorbed layer overlaps the reflectivity curve corresponding to the adsorption from a bulk solution with only PS80 at a concentration of 1.0 × cmc (Figure S2c). This is qualitatively similar to the dynamic tension data, in which the tension relaxation approaches the relaxation profile corresponding to the adsorbed layers from a solution with only excipient as the bulk concentration of the excipient increases, with an overlap at a concentration of 1.0 × cmc (cf. the comparison graph S2 in the Supporting Information) The EDP curves provide more quantitative information and demonstrate that the electron densities decrease as the bulk concentration of the excipient increases, a clear indication that in the competitive adsorption process the excipient is principally populating the surface and the surface concentration of the antibody is reduced (as opposed to an in-tandem adsorption as a second or multilayer). Similar observations can be made for the mAb-2 + PS80 mixture, where the reduction in the intensity of the mAb-2 peaks with increasing PS80 concentration indicated competitive adsorption (Figure 6c,d). However, in contrast with the dynamic tension relaxation data, it is—in the reflectivity or EDP curves—clear that for the lower surface activity antibody (mAb-2), only 0.2 × cmc is necessary to achieve overlap (see Figure S3b in the Supporting Information) and 1.0 × cmc is necessary to achieve overlap for mAb-1 (see Figure S2c in Supporting Information).

3.4. Calculation of Adsorbed Molecular Densities of mAb and Excipient from X-ray Reflectivity. *3.4.1. Adsorbed Layers of Polysorbate 80.* The surface concentration of PS80 (Γ_s or equivalently the area per molecule $\mathcal{A}_s = 1/\Gamma_s$) in the adsorbed layers derived from bulk solutions containing only the excipient is calculated from the EDPs of Figure 5c (see Supporting Information text). The EDPs for four concentrations were obtained, 0.05, 0.10, 0.20, and 1.0 × cmc. It is important to note that these EDPs represent the adsorption as obtained from 150 min from the formation of the air/water interface in the trough. As evident from the timescales for the dynamic tension relaxations, Figure 2b, these electron density distributions represent surface distributions at equilibrium or near equilibrium (i.e., a few mN/m from the equilibrium tension).

An approximate value for the thickness of the adsorbed PS80 layer can be obtained as the distance where the EDP profile reaches the electron density of pure water ($\rho_{e,w}$ = 0.333 electrons/Å^3). This thickness is ≈35−45 Å (Figure 5c) for PS80 and is not sensitive to concentration. Table 1 gives the surface concentrations (Γ_s) of PS80 as a function of bulk concentration, and we note that this concentration increases up to the cmc where it becomes constant. The error bars were calculated based on one standard deviation from the best-fit value. The values are in the range of 2.0−2.6 mg/m^2 for the concentration range of 0.05−1.0 × cmc. The equilibrium data of the tension against the bulk concentration can be fit using a Langmuir adsorption isotherm to obtain the maximum surface coverage (Γ_∞), and the value obtained (1.88 mg/m^2) is in approximate agreement with the coverage obtained at the cmc from the XR measurements (≈2.60 mg/m^2) (see Figure S1 and text in the Supporting Information).

3.4.2. Adsorbed Layers of mAbs. The surface concentrations of the adsorbed surface layers of mAb-1 and mAb-2 that are derived from the 0.5 mg/mL solutions are calculated from their EDPs (Figure 5d) (see Supporting Information text). The values are tabulated in Table 1 and are approximately 3.0 mg/m^2 for mAb-1 and 2.0 mg/m^2 for mAb-2. These values are in the range of (2−5 mg/m^2) based on the molecular orientation for a closed packed layer of mAbs at the air/water interface.[52,53] As expected from the dynamic tension curves, the surface concentration of mAb-2 is smaller than that of mAb-1 as mAb-2 is less surface-active. Note that the X-ray data show the difference in activity, as judged from the surface concentrations, to be quite large. The thicknesses of these antibody layers are approximately 140−150 Å, and from this dimension and the surface concentrations, the orientation of the antibodies in the adsorbed layer can be surmised to be side-on. The homology model (see Figure S4 and the Supporting Information text) of a single molecule of mAb-1 or mAb-2 showed that the dimensions of the molecule are 150 Å × 125 Å × 55 Å, and the Fab and Fc fragments have thicknesses of 40 and 55 Å, respectively. The molecular orientations that have been proposed for antibodies at a hydrophobic surface are end-on (Fab up or down relative to air), side-on, and flat-on (see Figure S5).[54] The values obtained for the area per molecule in Table 1 clearly suggest that it is not flat-on (150 × 125 = 18 750 Å^2) but the side-on (125 × 55 = 6875 Å^2) and end-on (150 × 55 = 8250 Å^2) that are in agreement with our calculated areas. As the thickness of the adsorbed mAb layers is in the range of 140−150 Å, the side-on configuration with a thickness of 150 Å is more likely than the end-on configuration with a thickness of 125 Å.

3.4.3. Mixed Adsorption Layers of mAb and PS80. Consider first the mixed surface layers derived from the bulk solutions of mAb-1 and PS80 (Table 2). The details for the calculation of the adsorbed amounts of mAb and PS80 during coadsorption are provided in the Supporting Information text. In all the EDPs reported (Figure 6b,d), the electron densities extend to 20 nm below the surface where the electron density

Table 1. Molecular Surface Concentrations for Pure Layers of mAb-1, mAb-2, and PS80

PS80 conc. × cmc	Γ_s (mg/m^2)	$\mathcal{A}_s$ (Å^2)
0.05	2.17 ± 0.05	100 ± 2
0.10	2.43 ± 0.04	90 ± 2
0.20	2.63 ± 0.09	83 ± 3
1.0	2.59 ± 0.12	84 ± 4
mAb 0.5 mg/mL	Γ_p (mg/m^2)	$\mathcal{A}_p$ (Å^2)
mAb-1	3.12 ± 0.04	7752 ± 95
mAb-2	2.33 ± 0.02	10417 ± 78

Table 2. Molecular Surface Concentrations in the Mixed Adsorbed Layers of mAb-1 and PS80

PS80 conc. × cmc	Γ_p (mg/m^2)	$\mathcal{A}_p$ (Å^2)	Γ_s (mg/m^2)	$\mathcal{A}_s$ (Å^2)
0.0	3.12 ± 0.04	7752 ± 95	0.0	
0.05	2.11 ± 0.12	11460 ± 696	0.70 ± 0.12	310 ± 44
0.10	1.41 ± 0.20	17104 ± 2813	1.33 ± 0.17	163 ± 18
0.15	0.37 ± 0.13	65907 ± 35827	2.24 ± 0.07	97 ± 3
0.20	0.12 ± 0.02	205460 ± 35159	2.53 ± 0.11	86 ± 4
1.0	0.04 ± 0.03		2.58 ± 0.10	84 ± 4

https://dx.doi.org/10.1021/acsami.9b21979
ACS Appl. Mater. Interfaces 2020, 12, 9977−9988

of bulk water ($\rho_{e,w}$ = 0.333 electrons/Å^3) is recovered. The area per molecule for an adsorbed layer of mAb-1 derived from a pure solution of mAb-1 is (7752 ± 95) Å^2. For a mixed layer derived from a solution with an mAb-1 concentration equal to 0.5 mg/mL and a low PS80 concentration equal to 0.05 × cmc, the area per molecule is (11 460 ± 696) Å^2/molecule for mAb-1 and (310 ± 44) Å^2/molecule for the surfactant. As the area per mAb molecule ($\mathcal{A}$) is the inverse of the surface concentration (Γ), these values indicate a lower adsorption of mAb-1 molecules relative to the pure mAb-1 system and an adsorption of PS80 molecules. Note, however, that the area per molecule of a pure layer of PS80 at this concentration is (100 ± 2) Å^2/molecule, so that the surfactant adsorption is not as high in the presence of the antibody because of the competitive adsorption. For the adsorbed layers derived from a solution of 0.10 × cmc PS80 and 0.5 mg/mL mAb-1, a further increase in the mAb-1 area to (17 104 ± 2813) Å^2/molecule is calculated, and a decrease in the surfactant area to (163 ± 18) Å^2/molecule is obtained. These values indicate that the adsorption of the antibody has been inhibited by a factor of 2 from the value for a pure layer of mAb-1. This trend continues with an increasing concentration of PS80 in the bulk solution. Although the adsorbed layers formed from a solution with PS80 at 0.20 × cmc and 0.5 mg/mL mAb-1 have a surfactant area per molecule nearly at the saturated value for a pure PS80 layer, the residual protein (205 460 Å^2/molecule) remains.

Based on Table 2, the minimum concentration of mAb measured using X-rays for mAb-1 (with the excipient concentration of 0.20 × cmc) in this study is around 0.12 mg/m^2. The error for this measurement was ± 0.02 mg/m^2. With a further increase in the PS80 solution concentration to 1.0 × cmc, there is no measurable mAb-1 on the surface, and the area per molecule of the surfactant is precisely its saturation value of (84 ± 4) Å^2, indicating a complete blocking of mAb-1 molecules to the air/water interface by the adsorption of the PS80 molecules. The error estimate for mAb-1 at the excipient concentration of 1.0 × cmc is equal to ± 0.03 mg/m^2. This suggests the minimum resolvable concentration, that is, the concentration at which the calculated value is of the order of the error, 0.04 ± 0.03 mg/m^2.

Similar trends are observed for the surface concentrations in the mixed adsorption layers derived from the competitive adsorption of mAb-2 and PS80 to the air/water interface (Table 3), and the excipient is once again able to completely block the adsorption of mAb to the surface for a large enough concentration of PS80. An important distinction, however, is that the minimum concentration of PS80 required for preventing the antibody (mAb-2) access to the surface is lower, 0.20 × cmc. At this concentration, the mAb-2 concentration is close to the minimum resolvable concentration of mAb, indicating no measurable amount of mAb-2 molecules on the surface, and the PS80 concentration has achieved its saturated value of (82 ± 2) Å^2/molecule. This conclusion was also reached by comparison of the XR curves (Figures S2c and S3b) for the mixed and pure systems. As mAb-1 is more surface-active than mAb-2, the excipient concentration needed to compete with the proteins should be higher. Thus, we conclude that to completely block the adsorption of these mAbs to the air/water interface, a PS80 concentration >1.0 × cmc is necessary for mAb-1 and >0.2 × cmc for mAb-2.

Table 3. Molecular Surface Concentrations in the Mixed Adsorbed Layers of mAb-2 and PS80

PS80 conc. × cmc	Γ_p (mg/m^2)	$\mathcal{A}_p$ (Å^2)	Γ_s (mg/m^2)	$\mathcal{A}_s$ (Å^2)
0.0	2.33 ± 0.02	10417 ± 78	0.0	
0.05	1.49 ± 0.09	16279 ± 1040	0.78 ± 0.11	278 ± 34
0.10	1.24 ± 0.01	19654 ± 146	1.14 ± 0.01	190 ± 2
0.15	1.13 ± 0.02	21442 ± 372	1.30 ± 0.04	167 ± 5
0.20	−0.01 ± 0.04		2.64 ± 0.07	82 ± 2
1.0	0.03 ± 0.03		2.58 ± 0.11	84 ± 5

4. COMPARISON BETWEEN PROTEINS AND MABS IN COMPETITIVE ADSORPTION WITH EXCIPIENTS

The results obtained in this study on the minimum concentration of PS80 necessary to inhibit the adsorption of mAb-1 and mAb-2 to an air/water interface can be compared to prior results that have measured the competitive adsorption of excipients and proteins other than mAbs to this interface, for example, BSA,[57,58] human serum albumin (HSA),[64] β-lactoglobulin,[60] and lysozyme,[66] as well as the flexible, nonglobular protein β-casein.[60−62] The competitive adsorption of each of these proteins has been studied with different excipients, namely, the phosphene oxides (decyl and dodecyl dimethyl phosphine oxide (C_{10}DMPO and C_{12}DMPO, respectively), SDS, and the polysorbates (PS80 and PS20). Table 4 lists these studies, giving the protein/surfactant pair, the bulk concentrations of the protein, and the concentration of excipient that was found to be sufficient to completely prevent the adsorption of the protein, as determined by dynamic surface tension or ellipsometry methods. Also tabulated in Table 4 is the molar ratio of the surfactant to protein that was measured to be sufficient to inhibit protein adsorption for the respective pair. The results of this study with mAb-1 and mAb-2 are also given in the table as well as three other studies on the competitive adsorption of mAbs and excipients to an air/water interface.[30,31,68] Relative to the mAbs, the molar ratio of the surfactant to the other (non-mAb) proteins which are necessary to inhibit protein adsorption is significantly higher (50−1000) than that for the mAbs (0.6−10). One potential reason is the relative flexibility of proteins to unfold and expose their hydrophobic patches upon adsorption to an air/water interface. The greater this flexibility to unfolding, the greater is the adsorption rate and the larger is the concentration of excipient necessary to outscale the protein for adsorption to the surface. Studies of the dynamic tensions of globular proteins (β-casein and lysozyme)[69,70] to an air/water interface indicate a rapid adsorption, which was attributed to the large flexibility in molecular arrangements. mAbs are less flexible, resulting in slower rates of kinetic adsorption and diffusional transport. Another factor that can be attributed to the flexibility of these molecules is the melting temperature that is tabulated in Table 4. mAbs generally have a higher melting temperature compared to other proteins that makes them relatively less flexible than the globular ones. This may explain the smaller ratios tabulated in Table 4. Other studies of the competitive adsorption of mAbs and excipient to an air/water interface also measure the same low range of concentrations of the excipient necessary to inhibit the adsorption of the mAbs. One consequence of this conclusion, important for pharmaceutical formulations, is that less excipient is necessary in the formulation to maintain the efficacy of mAb biologics.

https://dx.doi.org/10.1021/acsami.9b21979
ACS Appl. Mater. Interfaces 2020, 12, 9977−9988

Table 4. Comparison of the Amount of Surfactant Required to Inhibit the Adsorption of Proteins (Globular vs mAbs)

protein	molecular weight[55] kDa	melting point °C	surfactant	[protein] (mol/L) ×10^6	[surfactant] (mol/L) ×10^6	molar ratio [surfactant]/[protein]
BSA	66.8	65[56]	PS 80[57]	0.10	5	50
			PS 20[58]	3.74	80	21
β-casein	24	70[59]	C_{10}DMPO[60]	1.00	1000	1000
			C_{12}DMPO[60]	1.00	100	100
			C_{12}DMPO[61]	1.00	80	80
			SDS[62]	1.00	1000	1000
β-lactoglobulin	18.4	63[63]	C_{10}DMPO[60]	1.00	1000	1000
HSA	66.8	65[56]	C_{10}DMPO[64]	0.10	100	1000
lysozyme	14.3	75[65]	C_{10}DMPO[66]	0.70	200	286
			SDS[66]	0.70	5000	7000
IgG	150	73 and 80[67]	PS 80[31]	1.00	10	10
			PS 80[a]	3.33	2.4	0.72
			PS 80[a]	3.33	12	3.60
			PS 80[68]	0.35	1.2	3.48
			PS 20[30]	66.70	41	0.62

[a]This study; BSA: bovine serum albumin; HSA: human serum albumin; C_{10}DMPO: decyl dimethyl phosphine oxide; C_{12}DMPO: dodecyl dimethyl phosphine oxide; SDS: sodium dodecyl sulphate.

5. CONCLUSIONS

In this study, we have examined the competitive adsorption of a surfactant excipient and a monoclonal antibody (mAb) from a bulk solution to an air/water interface. We have established that the excipient can, at a sufficiently high bulk concentration, prevent the adsorption of the mAb directly to the air/water interface, and we have elucidated the effect of the surface activity of the mAb on the ability of the excipient to block the adsorption of the antibody. Dynamic surface tension measurements are consistent with the surface concentration values from the XR technique, confirming the higher surface activity of mAb-1 over mAb-2, and these techniques together can define the relative rates at which mAbs and the excipient molecules "race" and adsorb to the air/water interface.

These techniques have allowed us to postulate a mechanistic picture of competitive adsorption. At sufficiently lower concentrations of the excipient, the composition of molecules at the air/water interface was governed by the coadsorption of the mAb and excipient molecules. This coadsorption behavior continues until a critical excipient concentration can completely prevent the mAb adsorption. The XR measurements and the calculated surface concentrations of the excipient and mAb in the mixed adsorption layers showed that at a sufficiently high concentration of the excipient, the mAbs were completely blocked from adsorbing to the surface, and no measurable amount of mAb was detected on the surface or just beneath the air/water interface. For mAb-1, with a higher surface activity, a concentration of PS80 equal to the cmc was necessary to block the adsorption of the mAb, in agreement with the tension relaxation data. However, for mAb-2, with a lower activity, a lower concentration of PS80, 0.2 × cmc, a fivefold less concentration of excipient, was found to be necessary to completely block the adsorption of the mAb. This work indicates that the excipient can completely block the access of the mAb to the subsurface domain.

■ ASSOCIATED CONTENT

Supporting Information

The Supporting Information is available free of charge at https://pubs.acs.org/doi/10.1021/acsami.9b21979.

Langmuir adsorption fit for PS80; XR data analysis; surface concentration calculations for single component (PS80 or mAb) and mixed component (mAb + PS80); homology modeling and estimate of antibody size; structural orientation of mAbs on surface adsorption; cmc of PS80 using Langmuir adsorption fit; comparison of XR measurements by overlapping the mixed component and the corresponding pure surfactant XR data; visualization of the mAb structure and dimensions of a representative IgG molecule; possible orientations of a representative IgG molecule at the air/water interface; and the normalized XR and EDP profiles using the model-independent and the slab model (PDF)

■ AUTHOR INFORMATION

Corresponding Authors

Charles Maldarelli − *Department of Chemical Engineering and Levich Institute, The City College of New York, New York, New York 10031, United States;* orcid.org/0000-0001-7427-2349; Email: cmaldarelli@ccny.cuny.edu

Raymond S. Tu − *Department of Chemical Engineering, The City College of New York, New York, New York 10031, United States;* orcid.org/0000-0002-6192-7665; Email: tu@ccny.cuny.edu

Authors

Ankit D. Kanthe − *Department of Chemical Engineering, The City College of New York, New York, New York 10031, United States;* orcid.org/0000-0003-4451-5383

Mary Krause − *Drug Product Science and Technology, Bristol-Myers Squibb, New Brunswick, New Jersey 08901, United States;* orcid.org/0000-0002-3299-5423

Songyan Zheng − *Drug Product Science and Technology, Bristol-Myers Squibb, New Brunswick, New Jersey 08901, United States*

Andrew Ilott − *Drug Product Science and Technology, Bristol-Myers Squibb, New Brunswick, New Jersey 08901, United States*

Jinjiang Li − *Drug Product Science and Technology, Bristol-Myers Squibb, New Brunswick, New Jersey 08901, United States*

https://dx.doi.org/10.1021/acsami.9b21979
ACS Appl. Mater. Interfaces 2020, 12, 9977−9988

Wei Bu − *ChemMatCARS, Center for Advanced Radiation Sources, University of Chicago, Chicago, Illinois 60637, United States*

Mrinal K. Bera − *ChemMatCARS, Center for Advanced Radiation Sources, University of Chicago, Chicago, Illinois 60637, United States*

Binhua Lin − *ChemMatCARS, Center for Advanced Radiation Sources, University of Chicago, Chicago, Illinois 60637, United States;* orcid.org/0000-0001-5932-4905

Complete contact information is available at: https://pubs.acs.org/10.1021/acsami.9b21979

Notes

The authors declare no competing financial interest.

■ ACKNOWLEDGMENTS

We acknowledge the financial support from Bristol Myers Squibb Co. For this research, XR measurements were conducted at NSF's ChemMatCARS Sector 15 that is principally supported by the Divisions of Chemistry (CHE) and Materials Research (DMR), NSF, under grant number NSF/CHE-1834750. Use of the Advanced Photon Source (APS), an Office of Science User Facility operated for the U.S. Department of Energy (DOE) Office of Science by Argonne National Laboratory (ANL), was supported by the U.S. DOE under contract no. DE-AC02-06CH11357. C.M. and R.S.T. thank Dr. Joe Strzalka, Beamline Scientist, Sector 8, APS, ANL, for his insights on the modeling of the XR data. R.S.T. thanks the support of the National Science Foundation under Grant No. 1605904.

■ REFERENCES

(1) Zhang, Q.; Chen, G.; Liu, X.; Qian, Q. Monoclonal Antibodies as Therapeutic Agents in Oncology and Antibody Gene Therapy. *Cell Res.* **2007**, *17*, 89−99.

(2) Lee, H. J.; McAuley, A.; Schilke, K. F.; McGuire, J. Molecular Origins of Surfactant-Mediated Stabilization of Protein Drugs. *Adv. Drug Delivery Rev.* **2011**, *63*, 1160−1171.

(3) Wang, X.; Das, T. K.; Singh, S. K.; Kumar, S. Potential aggregation prone regions in biotherapeutics. *mAbs* **2009**, *1*, 254−267.

(4) Wang, W. Protein Aggregation and its Inhibition in Biopharmaceutics. *Int. J. Pharm.* **2005**, *289*, 1−30.

(5) Wang, W.; Nema, S.; Teagarden, D. Protein Aggregation-Pathways and Influencing Factors. *Int. J. Pharm.* **2010**, *390*, 89−99.

(6) Weiss, W. F.; Young, T. M.; Roberts, C. J. Principles, Approaches, and Challenges for Predicting Protein Aggregation Rates and Shelf Life. *J. Pharm. Sci.* **2009**, *98*, 1246−1277.

(7) Ghazvini, S.; Kalonia, C.; Volkin, D. B.; Dhar, P. Evaluating the Role of the Air-Solution Interface on the Mechanism of Subvisible Particle Formation Caused by Mechanical Agitation for an IgG1 mAb. *J. Pharm. Sci.* **2016**, *105*, 1643−1656.

(8) Koepf, E.; Eisele, S.; Schroeder, R.; Brezesinski, G.; Friess, W. Notorious But Not Understood: How Liquid-Air Interfacial Stress Triggers Protein Aggregation. *Int. J. Pharm.* **2018**, *537*, 202−212.

(9) Heitz, F.; Van Mau, N. Protein Structural Changes Induced by their Uptake at Interfaces. *Biochim. Biophys. Acta, Protein Struct. Mol. Enzymol.* **2002**, *1597*, 1−11.

(10) Yano, Y. F.; Uruga, T.; Tanida, H.; Toyokawa, H.; Terada, Y.; Takagaki, M.; Yamada, H. Driving Force Behind Adsorption-Induced Protein Unfolding : A Time-Resolved X-ray Reflectivity Study on Lysozyme Adsorbed at an Air. *Langmuir* **2009**, *25*, 32−35.

(11) Yano, Y. F. Kinetics of Protein Unfolding at Interfaces. *J. Phys.: Condens. Matter* **2012**, *24*, 503101.

(12) Chang, B. S. *Formulation and Process Development Strategies for Manufacturing Biopharmaceuticals*; John Wiley and Sons, Inc.: Hoboken, New Jersey, 2010.

(13) Harrison, J. S.; Gill, A.; Hoare, M. Stability of a Single-Chain Fv Antibody Fragment when Exposed to a High Shear Environment Combined with Air-Liquid Interfaces. *Biotechnol. Bioeng.* **1998**, *59*, 517−519.

(14) Richter, A. G.; Kuzmenko, I. Using In Situ X-Ray Reflectivity to Study Protein Adsorption on Hydrophilic and Hydrophobic Surfaces: Benefits and Limitations. *Langmuir* **2013**, *29*, 5167−5180.

(15) Rosenberg, A. S. Effects of Protein Aggregates: An Immunologic Perspective. *AAPS J.* **2006**, *8*, E501−E507.

(16) Martin, A. H.; Meinders, M. B. J.; Bos, M. A.; Cohen Stuart, M. A.; Van Vliet, T. Conformational Aspects of Proteins at The Air/Water Interface Studied by Infrared Reflection-Absorption Spectroscopy. *Langmuir* **2003**, *19*, 2922−2928.

(17) Vázquez-Rey, M.; Lang, D. A. Aggregates in Monoclonal Antibody Manufacturing Processes. *Biotechnol. Bioeng.* **2011**, *108*, 1494−1508.

(18) Kapp, S. J.; Larsson, I.; Van De Weert, M.; Cárdenas, M.; Jorgensen, L. Competitive Adsorption of Monoclonal Antibodies and Nonionic Surfactants at Solid Hydrophobic Surfaces. *J. Pharm. Sci.* **2015**, *104*, 593−601.

(19) Ohtake, S.; Kita, Y.; Arakawa, T. Interactions of Formulation Excipients with Proteins in Solution and in the Dried State. *Adv. Drug Delivery Rev.* **2011**, *63*, 1053−1073.

(20) Singh, S. M.; Bandi, S.; Jones, D. N. M.; Mallela, K. M. G. Effect of Polysorbate 20 and Polysorbate 80 on the Higher-Order Structure of a Monoclonal Antibody and its Fab and Fc Fragments Probed Using 2D Nuclear Magnetic Resonance Spectroscopy. *J. Pharm. Sci.* **2017**, *106*, 3486−3498.

(21) Khan, T. A.; Mahler, H.-C.; Kishore, R. S. K. Key Interactions of Surfactants in Therapeutic Protein Formulations: A Review. *Eur. J. Pharm. Biopharm.* **2015**, *97*, 60−67.

(22) Joshi, O.; Chu, L.; McGuire, J.; Wang, D. Q. Adsorption and Function of Recombinant Factor VIII at the Air-Water Interface In the Presence of Tween 80. *J. Pharm. Sci.* **2009**, *98*, 3099−3107.

(23) Krägel, J.; Wüstneck, R.; Clark, D.; Wilde, P.; Miller, R. Dynamic Surface Tension and Surface Shear Rheology Studies of Mixed -Lactoglobulin/Tween 20 Systems. *Colloids Surf., A* **1995**, *98*, 127−135.

(24) Krielgaard, L.; Jones, L. S.; Randolph, T. W.; Frokjaer, S.; Flink, J. M.; Manning, M. C.; Carpenter, J. F. Effect of Tween 20 on Freeze-Thawing- and Agitation-Induced Aggregation of Recombinant Human Factor XIII. *J. Pharm. Sci.* **1998**, *87*, 1597−1603.

(25) McClellan, S. J.; Franses, E. I. Exclusion of Bovine Serum Albumin from the Air/Water Interface by Sodium Myristate. *Colloids Surf., B* **2003**, *30*, 1−11.

(26) Chen, P.; Prokop, R. M.; Susnar, S. S.; Neumann, A. W. Interfacial Tensions of Protein Solutions Using Axisymmetric Drop Shape Analysis. *Stud. Interface Sci.* **1998**, *7*, 303−339.

(27) Liao, Z.; Lampe, J. W.; Ayyaswamy, P. S.; Eckmann, D. M.; Dmochowski, I. J. Protein Assembly at the Air-Water Interface Studied by Fluorescence Microscopy. *Langmuir* **2011**, *27*, 12775−12781.

(28) Noskov, B. A.; Krycki, M. M. Formation of Protein/Surfactant Adsorption Layer as Studied by Dilational Surface Rheology. *Adv. Colloid Interface Sci.* **2017**, *247*, 81−99.

(29) Niño, M. R. R.; Patino, J. M. R. Surface Tension of Bovine Serum Albumin and Tween 20 at the Air-Aqueous Interface. *J. Am. Oil Chem. Soc.* **1998**, *75*, 1241−1248.

(30) Mahler, H.-C.; Senner, F.; Maeder, K.; Mueller, R. Surface Activity of a Monoclonal Antibody. *J. Pharm. Sci.* **2009**, *98*, 4525−4533.

(31) Serno, T.; Härtl, E.; Besheer, A.; Miller, R.; Winter, G. The Role of Polysorbate 80 and HPCD at the Air-Water Interface of IgG Solutions. *Pharm. Res.* **2013**, *30*, 117−130.

(32) Pershan, P. S.; Schlossman, M. *Liquid Surfaces and Interfaces: Synchrotron X-ray Methods*; Cambridge University Press: Cambridge, 2012.
(33) Tolan, M. *X-ray Scattering from Soft-Matter Thin Films*; Springer, 1988.
(34) Harzallah, B.; Aguié-Béghin, V.; Douillard, R.; Bosio, L. A Structural Study of β-Casein Adsorbed Layers at the Air-Water Interface Using X-ray and Neutron Reflectivity. *Int. J. Biol. Macromol.* **1998**, *23*, 73−84.
(35) Evers, F.; Shokuie, K.; Paulus, M.; Sternemann, C.; Czeslik, C.; Tolan, M. Exploring the Interfacial Structure of Protein Adsorbates and the Kinetics of Protein Adsorption: An In Situ High-Energy X-Ray Reflectivity Study. *Langmuir* **2008**, *24*, 10216−10221.
(36) Petrash, S.; Liebmann-Vinson, A.; Foster, M. D.; Lander, L. M.; Brittain, W. J.; Majkrzak, C. F. Neutron and X-Ray Reflectivity Studies of Human Serum Albumin Adsorption onto Functionalized Surfaces of Self-Assembled Monolayers. *Biotechnol. Prog.* **1997**, *13*, 635−639.
(37) Sheller, N. B.; Petrash, S.; Foster, M. D.; Tsukruk, V. V. Atomic Force Microscopy and X-ray Reflectivity Studies of Albumin Adsorbed onto Self-Assembled Monolayers of Hexadecyltrichlorosilane. *Langmuir* **1998**, *14*, 4535−4544.
(38) Lin, B.; Meron, M.; Gebhardt, J.; Graber, T.; Schlossman, M. L.; Viccaro, P. J. The Liquid Surface/Interface Spectrometer at ChemMatCARS Synchrotron Facility at the Advanced Photon Source. *Phys. B* **2003**, *336*, 75−80.
(39) Schlossman, M. L.; Synal, D.; Guan, Y.; Meron, M.; Shea-McCarthy, G.; Huang, Z.; Acero, A.; Williams, S. M.; Rice, S. A.; Viccaro, P. J. A Synchrotron X-ray Liquid Surface Spectrometer. *Rev. Sci. Instrum.* **1997**, *68*, 4372−4384.
(40) Kerwin, B. A. Polysorbates 20 and 80 Used in the Formulation of Protein Biotherapeutics: Structure and Degradation Pathways. *J. Pharm. Sci.* **2008**, *97*, 2924−2935.
(41) Chang, C.-H.; Franses, E. I. "A dsorption dynamics of surfactants at the air/water interface: a critical review of mathematical models, data, and mechanisms". *Colloids Surf., A* **1995**, *100*, 1−45.
(42) Bos, M. A.; van Vliet, T. Interfacial Rheological Properties of Adsorbed Protein Layers and Surfactants: A Review. *Adv. Colloid Interface Sci.* **2001**, *91*, 437−471.
(43) Kannan, A.; Shieh, I. C.; Leiske, D. L.; Fuller, G. G. Monoclonal Antibody Interfaces: Dilatation Mechanics and Bubble Coalescence. *Langmuir* **2018**, *34*, 630−638.
(44) Maldonado-Valderrama, J.; Wege, H. A.; Rodríguez-Valverde, M. A.; Gálvez-Ruiz, M. J.; Cabrerizo-Vílchez, M. A. Comparative Study of Adsorbed and Spread β-Casein Monolayers at the Water-Air Interface with the Pendant Drop Technique. *Langmuir* **2003**, *19*, 8436−8442.
(45) Mellema, M.; Clark, D. C.; Husband, F. A.; Mackie, A. R. Water Interface as Supported by Surface Rheological Measurements. *Langmuir* **1998**, *14*, 1753−1758.
(46) Leiske, D. L.; Shieh, I. C.; Tse, M. L. A Method to Measure Protein Unfolding at an Air-Liquid Interface. *Langmuir* **2016**, *32*, 9930−9937.
(47) Shieh, I. C.; Patel, A. R. Predicting the Agitation-Induced Aggregation of Monoclonal Antibodies Using Surface Tensiometry. *Mol. Pharm.* **2015**, *12*, 3184−3193.
(48) Chennamsetty, N.; Voynov, V.; Kayser, V.; Helk, B.; Trout, B. L. Design of Therapeutic Proteins with Enhanced Stability. *Proc. Natl. Acad. Sci. U.S.A.* **2009**, *106*, 11937−11942.
(49) Zheng, S.; Adams, M.; Mantri, R. V. An Approach to Mitigate Particle Formation on the Dilution of a Monoclonal Antibody Drug Product in an IV Administration Fluid. *J. Pharm. Sci.* **2016**, *105*, 1349−1350.
(50) Li, J.; Krause, M. E.; Chen, X.; Cheng, Y.; Dai, W.; Hill, J. J.; Huang, M.; Jordan, S.; LaCasse, D.; Narhi, L.; Shalaev, E.; Shieh, I. C.; Thomas, J. C.; Tu, R.; Zheng, S.; Zhu, L. Interfacial Stress in the Development of Biologics: Fundamental Understanding, Current Practice, and Future Perspective. *AAPS J.* **2019**, *21*, 44.
(51) Bu, W.; Yu, H.; Luo, G.; Bera, M. K.; Hou, B.; Schuman, A. W.; Lin, B.; Meron, M.; Kuzmenko, I.; Antonio, M. R.; Soderholm, L.; Schlossman, M. L. Observation of A Rare Earth Ion-Extractant Complex Arrested at the Oil-Water Interface During Solvent Extraction. *J. Phys. Chem. B* **2014**, *118*, 10662−10674.
(52) Baszkin, A.; Boissonnade, M. M.; Kamyshny, A.; Magdassi, S. Native and Hydrophobically Modified Human Immunoglobulin G at the Air/Water Interface: Sequential and Competitive Adsorption. *J. Colloid Interface Sci.* **2001**, *239*, 1−9.
(53) Buijs, J.; Lichtenbelt, J. W. T.; Norde, W.; Lyklema, J. Adsorption of Monoclonal IgGs and their F(Ab′)2 Fragments onto Polymeric Surfaces. *Colloids Surf., B* **1995**, *5*, 11−23.
(54) Wiseman, M. E.; Frank, C. W. Antibody Adsorption and Orientation on Hydrophobic Surfaces. *Langmuir* **2012**, *28*, 1765−1774.
(55) Chalikian, T. V.; Totrov, M.; Abagyan, R.; Breslauer, K. J. The Hydration of Globular Proteins as Derived from Volume and Compressibility Measurements: Cross Correlating Thermodynamic and Structural Data. *J. Mol. Biol.* **1996**, *260*, 588−603.
(56) Molodenskiy, D.; Shirshin, E.; Tikhonova, T.; Gruzinov, A.; Peters, G.; Spinozzi, F. Thermally Induced Conformational Changes and Protein−Protein Interactions of Bovine Serum Albumin in Aqueous Solution Under Different ph and Ionic Strengths as Revealed by SAXS Measurements. *Phys. Chem. Chem. Phys.* **2017**, *19*, 17143−17155.
(57) Grigoriev, D.; Derkatch, S.; Kragel, J.; Miller, R. Relationship Between Structure and Rheological Properties of Mixed BSA/Tween 80 Adsorption Layers at the Air/Water Interface. *Food Hydrocolloids* **2007**, *21*, 823−830.
(58) Wu, D.; Xu, G. Y.; Liu, J.; Li, Y. M. Investigation on Adsorption Dynamics of Protein/Tween-20 Mixture at the Surface of Solution by Surface Pressure Measurement. *J. Dispersion Sci. Technol.* **2006**, *27*, 523−526.
(59) Farrell, H. M.; Qi, P.; Wickham, E.; Unruh, J. Secondary Structural Studies of Bovine Caseins: Structure and Temperature Dependence of β-Casein Phosphopeptide (1-25) as Analyzed by Circular Dichroism, FTIR Spectroscopy, and Analytical Ultracentrifugation. *J. Protein Chem.* **2002**, *21*, 307−321.
(60) Kotsmar, C.; Grigoriev, D. O.; Xu, F.; Aksenenko, E. V.; Fainerman, V. B.; Leser, M. E.; Miller, R. Equilibrium of Adsorption of Mixed Milk Protein/Surfactant Solutions at the Water/Air Interface. *Langmuir* **2008**, *24*, 13977−13984.
(61) Kotsmár, C.; Grigoriev, D. O.; Makievski, A. V.; Ferri, J. K.; Krägel, J.; Miller, R.; Möhwald, H. Drop Profile Analysis Tensiometry with Drop Bulk Exchange to Study the Sequential and Simultaneous Adsorption of A Mixed ″-casein/C12DMPO system. *Colloid Polym. Sci.* **2008**, *286*, 1071−1077.
(62) Dan, A.; Kotsmar, C.; Ferri, J. K.; Javadi, A.; Karbaschi, M.; Krägel, J.; Wüstneck, R.; Miller, R. Mixed Protein−Surfactant Adsorption Layers Formed in A Sequential and Simultaneous Way at Water−Air and Water−Oil Interfaces. *Soft Matter* **2012**, *8*, 6057−6065.
(63) Prabakaran, S.; Damodaran, S. Thermal Unfolding of β-Lactoglobulin: Characterization of Initial Unfolding Events Responsible for Heat-Induced Aggregation. *J. Agric. Food Chem.* **1997**, *45*, 4303−4308.
(64) Miller, R.; Fainerman, V. B.; Makievski, A. V.; Krägel, J.; Grigoriev, D. O.; Kazakov, V. N.; Sinyachenko, O. V. Dynamics of Protein and Mixed Protein/Surfactant Adsorption Layers at the Water/Fluid Interface. *Adv. Colloid Interface Sci.* **2000**, *86*, 39−82.
(65) Sassi, P.; Giugliarelli, A.; Paolantoni, M.; Morresi, A.; Onori, G. Unfolding and Aggregation of Lysozyme: A Thermodynamic and Kinetic Study by FTIR Spectroscopy. *Biophys. Chem.* **2011**, *158*, 46−53.
(66) Alahverdjieva, V. S.; Grigoriev, D. O.; Fainerman, V. B.; Aksenenko, E. V.; Miller, R.; Möhwald, H. Competitive Adsorption from Mixed Hen Egg-White Lysozyme/Surfactant Solutions at the Air−Water Interface Studied by Tensiometry, Ellipsometry, and Surface Dilational Rheology. *J. Phys. Chem. B* **2008**, *112*, 2136−2143.
(67) Rubin, J.; Sharma, A.; Linden, L.; Bommarius, A. S.; Behrens, S. H. Gauging Colloidal and Thermal Stability in Human Igg1−Sugar

https://dx.doi.org/10.1021/acsami.9b21979
ACS Appl. Mater. Interfaces 2020, 12, 9977−9988

Solutions Through Diffusivity Measurements. *J. Phys. Chem. B* **2014**, *118*, 2803−2809.
(68) Smith, C.; Li, Z.; Holman, R.; Pan, F.; Campbell, R. A.; Campana, M.; Li, P.; Webster, J. R. P.; Bishop, S.; Narwal, R.; Uddin, S.; van der Walle, C. F.; Lu, J. R. Antibody Adsorption on the Surface of Water Studied by Neutron Reflection. *Mabs* **2017**, *9*, 466−475.
(69) Alahverdjieva, V. S.; Grigoriev, D. O.; Ferri, J. K.; Fainerman, V. B.; Aksenenko, E. V.; Leser, M. E.; Michel, M.; Miller, R. Adsorption Behaviour of Hen Egg-White Lysozyme at the Air/Water Interface. *Colloids Surf., A* **2008**, *323*, 167−174.
(70) Mackie, A. R.; Gunning, A. P.; Ridout, M. J.; Wilde, P. J.; Morris, V. J. Orogenic Displacement in Mixed *β*-Lactoglobulin/*β*-Casein films at the air/water interface. *Langmuir* **2001**, *17*, 6593−6598.

https://dx.doi.org/10.1021/acsami.9b21979
ACS Appl. Mater. Interfaces 2020, 12, 9977−9988